1 Introduction

Equipment design for the process industry requires proper understanding of the fluid dynamics which in turn often relies on experimental investigation of three dimensional and frequently multiphase flow fields. The parameters of interest are velocity, phase and or species concentration and temperature distribution throughout the flow field. Although traditional measuring methods based on the use of probes have the ability to provide accurate measurements with fine time resolution, such probes are not only intrusive but they also need to be moved through the volume of the system being studied in order to map the entire flow field. Methods that have the ability to provide the relevant measurements throughout the flow field without disturbing the flow are clearly advantageous. Computed Tomography (CT) is one such technique that is capable of providing the concentration, or the holdup distribution, of the phases in multiphase systems. The advantage of tomography lies in its noninvasiveness and in the ability to obtain the parameters of interest over an entire cross section of the flow field of interest. If several such individual layers, each with their measured distribution are stacked up, a three dimensional field can be reconstructed. The void fraction, and its distribution, in a two phase flow system are important in determining the interfacial area available for heat and mass transfer between the phases. The characterization of inhomogeneous two phase flow fields is complete only when the holdup and its distribution are also measured in addition to other hydrodynamic quantities such as phase velocity.

Tomography has been in use in the medical field for diagnostic radiology for more than 50 years. However, the application of tomography to engineering applications is relatively recent (mid-1980's). Applications range from nondestructive testing of manufactured components (Del Grande et al., 1993, Martz et al., 1993), the investigation of process equipment (process tomography) (Dickin et al., 1993), to underground imaging in relation to environmental remediation of contaminated soil and groundwater (Daily and Ramirez, 1995). In the process industry, tomography aids in the characterization of the flow in chemical reactors, which is essential in providing an accurate basis for modeling of the reaction processes involved. In these systems, the phases (especially a solid phase) involved are opaque and prevent the use of optical techniques for the measurement of flow parameters. Thus, tomography in its various forms provides the only means to obtain the required information.

Although in the medical field tomography is largely based on the use of high energy electromagnetic radiation such as X-rays and gamma rays, for engineering applications a number of other forms of tomography have evolved. These include tomography based on the use of ultrasound, impedance (capacitance), and even visible light. The methods based on the use of gamma rays can be classified into emission and transmission tomography. In emission tomography the geometric distribution of the activity of radionuclides introduced

into the system is imaged. One encounters positron emission tomography and single photon emission tomography depending upon the kind of radiation used. Both are extensively used in medical imaging. Transmission tomography, on the other hand, is based on the principle of measuring the attenuation of a beam of radiation transmitted through the object. Based on a number of such attenuation measurements along several paths through the object, an image of the absorption coefficients within the scanned section is reconstructed. Phase holdup and its distribution can be derived from the absorption coefficient distribution for a two phase flow system, since the absorption coefficients are a function of the type of material traversed by the beam of radiation. In ultrasonic tomography, the gas bubbles are considered to be opaque plates that absorb sound. The large difference in the ultrasonic impedance between a gas and a liquid phase serves as a means for discriminating between the phases. Impedance tomography is based on measuring the electrical resistance, or the dielectric permittivity, in the flow between pairs of electrodes, a number of which are evenly spaced around the test section. Although both ultrasonic and impedance tomography have the advantage of being capable of fine temporal resolution, the achievable spatial resolution is rather coarse owing to the measurements being affected by the holdup distribution as well as by a number of other parameters such as the electrical properties and temperature of the medium. X-ray and gamma ray tomography on the other hand are capable of high spatial resolution but temporal resolution is limited by the activity of the source used. Use of a higher activity source, or a X-ray tube with a higher power output, is constrained by radiation safety considerations. Thus, most often, with these systems the measurements of the concentration or holdup that is obtained is time averaged.

The focus of this report is on gamma and X-ray transmission tomography. We begin by first discussing the basic principles of tomography. The different hardware configurations for arranging the radiation detectors and the source of radiation, as well as the methods for measuring the attenuation are described. The various mathematical methods used for reconstruction of the density distribution from the attenuation measurements as well as a comparison between the various methods are then presented. Finally, the application of computed tomography for the experimental investigation of multiphase systems is illustrated through a few examples and some possible industrial and process applications are outlined. In presenting the above material we highlight our own experience in implementing a tomographic system for holdup measurements in two phase flow systems such as bubble columns and fluidized beds.

2 Technical Aspects of Computed Tomography

2.1 Basic Principle

A narrow beam of radiation traversing a straight path through an object gets attenuated primarily by absorption and to a lesser extent by scattering. If the object were to be divided into a number of elements, then the problem in CT is to determine the extent to which the material in each element attenuates the beam, and to display this information in the form of an image.

The intensity of a beam of monoenergetic radiation that is transmitted through a homogeneous material is governed by the Beer-Lambert's law which can be expressed as:

$$T = \frac{I}{I_o} = e^{-\rho \mu l} \tag{1}$$

where T is the transmission ratio, I_o the incident radiation, I the detected radiation, μ the mass attenuation coefficient, ρ the medium density, and l the path length through the medium. The product $\mu\,\rho$ is defined as the linear attenuation coefficient of the medium and is the ratio of the percentage change in the flux of the beam to the change in distance as the beam traverses the medium (Newton and Potts, 1981). The product $\mu\rho l$ is referred to as the absorptance of the medium. If the medium is made of two materials of mass attenuation coefficients μ_1 and μ_2, densities ρ_1 and ρ_2, and thickness l_1 and l_2, respectively, the net absorptance, A, is:

$$A = \rho_1 \mu_1 l_1 + \rho_2 \mu_2 l_2 \tag{2}$$

If $l_1 = \epsilon_1 L$ and $l_2 = (1 - \epsilon_1) L$, where $L = l_1 + l_2$, then:

$$A = [\rho_1 \mu_1 \epsilon_1 + \rho_2 \mu_2 (1 - \epsilon_1)] L \tag{3}$$

where ϵ_1 is the void fraction of one of the phases.

The measured quantity $ln\, I_o/I$ is the net absorbance and is the integral sum of the attenuation coefficients of the material along the incident line. A single measurement of the attenuation can be used to compute ϵ_1, the fraction of the medium along the beam path that is occupied by material one. The information obtained is global (averaged along the path), and no information can be obtained regarding the composition of the medium locally. Since the attenuations along a beam path vary considerably, a large number of such attenuation measurements of the object must be obtained from many directions to determine the attenuation coefficient of each element (for a two dimensional slice of the object the element is called a pixel). This measurement followed by a mathematical procedure

for computing the attenuation coefficients of the pixels constitutes the basic idea behind tomography. Since the reconstruction process is performed by using a computer, and since the process of data collection is automated by interfacing the hardware to a computer, the process is popularly referred to either as Computer Assisted Tomography (CAT) or as Computed Tomography (CT).

2.2 CT Scanning Modes

Scanners for transmission tomography have some source of radiation, such as an X-ray tube or an encapsulated gamma ray source, positioned on one side of the object to be scanned and a detector or a set of detectors arranged on the other side. Transmission measurements of a collimated beam of radiation are obtained along several paths from many directions around the object to cover the cross section as uniformly as possible. The term 'CT scanning modes' refers to the geometrical arrangement of the combination of the detectors (or detector) and the source of radiation, and the method adopted for acquiring the data for the requisite number of projections. In principle, it involves rotating the source-detector arrangement synchronously with respect to the test section.

There are three methods of scanning that are commonly used. The simplest of these is parallel scanning in which a source, emitting a single pencil beam of radiation, and a detector are coupled together so that the detector is always facing the source as illustrated in Fig. 1(a). For obtaining a single view, the source and detector move on opposite sides of the test section measuring the absorptance (also called attenuation) at each position i. e. along the chord that connects the detector and the source. For the next view, the detector source arrangement rotates about the test section and the translation is repeated. This method of scanning is very time consuming. The other two methods result in rapid collection of the data. The second method has an array of detectors facing a single source. The source is collimated in such a way that the pattern of the beam is a fan with a thickness of about 5 to 10 mm (Fig. 1(b)). A single view is obtained for a given position of the source-detector arrangement, which is then rotated to get the next view. Another method, referred to as the fourth generation scanning configuration, is the fixed detector-rotating source arrangement in which a large number of detectors are mounted on a fixed ring as shown in Fig. 1(c). Inside this ring a fan beam source rotates around the test section, and the outputs of the detectors facing the source are sampled every few milliseconds. All such samples for any one detector are referred to as a detector-vortex fan and constitute one view of the object.

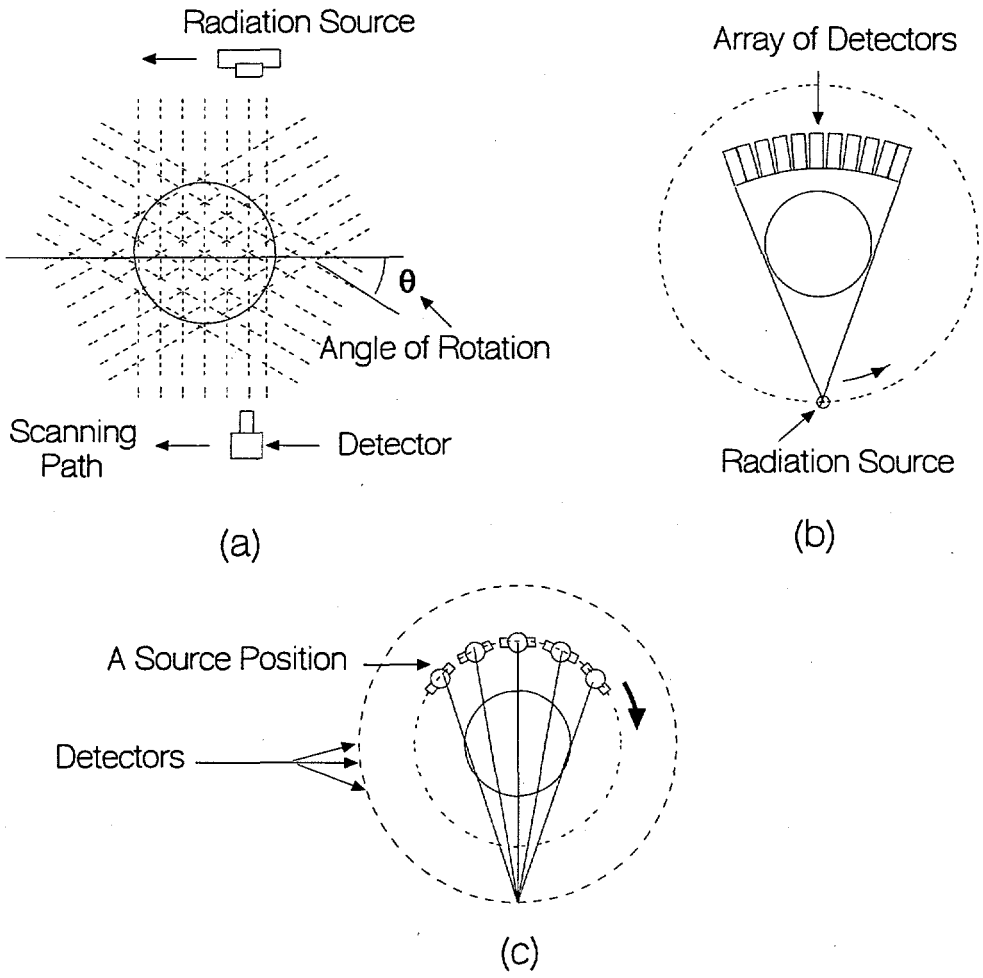

Figure 1: CT scanning modes, (a) Parallel beam scanning mode, (b) Rotating fan beam scanning mode, (c) Fixed detector-rotating source scanning mode.

2.3 Image Reconstruction from Projections

Given a set of projections (ray sums), the next step is to reconstruct the attenuation coefficient distribution (image). Equation (3) for the absorptance can be written in a more general form as:

$$P(l,\theta) = \int_L f(x,y)ds \tag{4}$$

where $P(l,\theta)$ called the projection is the integral of the attenuation coefficients along the path L, $f(x,y)$ represents the image function and L indicates the line over which the integral is obtained. The basic problem then is, the inversion of an integral equation along a linear path through a scalar field. Radon (1917) showed that a function with finite support, continuous and having continuous first derivatives, can be uniquely reconstructed from an infinite set of line integrals in the form of Eq. (4). The solution, known as the Radon transform, is given by:

$$f(x,y) = \frac{1}{4\pi^2}\int_0^{2\pi}\int_{-\infty}^{\infty}\frac{-1}{l - x\,Cos\,\theta - y\,Sin\,\theta}\frac{\partial P(l,\theta)}{\partial l}\,dl\,d\theta \tag{5}$$

where $(l - x\,Cos\,\theta - y\,Sin\,\theta)$ is the perpendicular distance of the point (x,y) from the line l, and $P(l,\theta)$ is the integral of $f(x,y)$ along line l (ref. Fig. 2). Utilization of the Radon transform for image reconstruction is possible only in theory since it calls for an infinite number of noiseless projection measurements. In practice, methods that approximate the Radon's transform in some sense are used. Many different types of algorithms are available for the reconstruction process and the principle behind the important ones are briefly presented in what follows.

The integral transformation method of reconstruction is based on approximating the inverse Radon transform. The essential steps in obtaining the inverse Radon transform of a function of two variables are :

1. Partial differentiation of the function with respect to its first variable to obtain another function q.

2. q is Hilbert transformed with respect to its first variable to obtain a function t. Thus if q is a function of two variables, l and θ, for any real number pair (l',θ), the Hilbert transform is defined as :

$$[Hq](l',\theta) = -\frac{1}{\pi}\int_{-\infty}^{\infty}\frac{q(l,\theta)}{l' - l}\,dl$$

   The improper integral needs to be evaluated in the Cauchy principle value sense.

3. t is then backprojected onto the original function domain. Given a function t of two variables, its backprojected function $[Bt]$ is a function of two polar variables defined

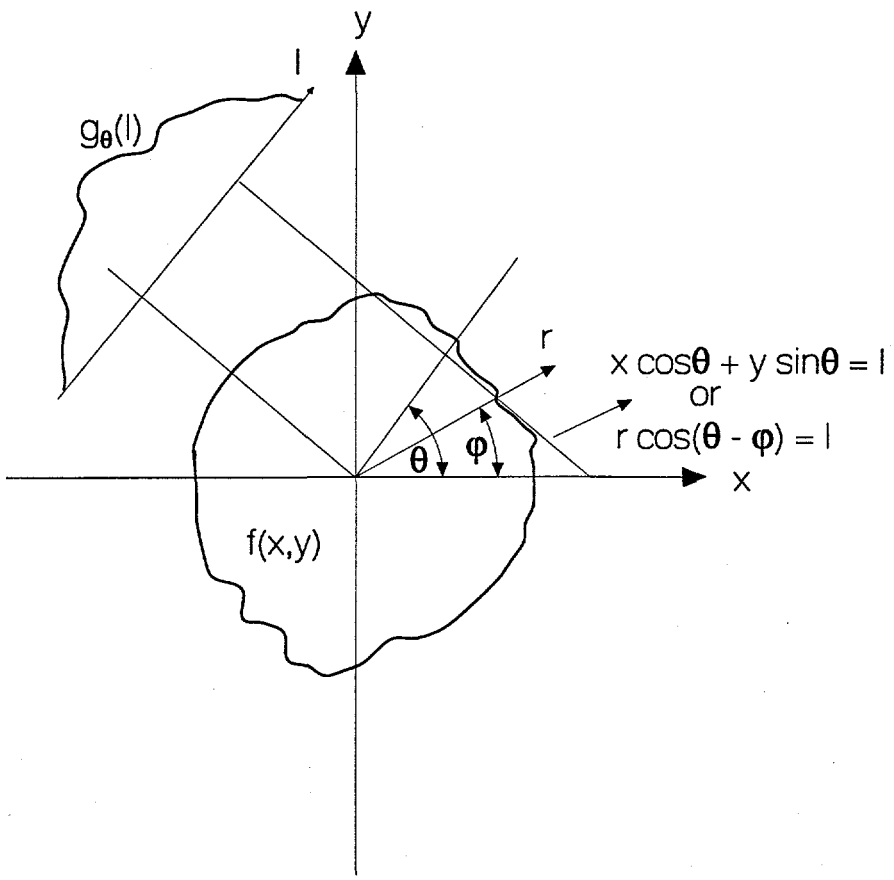

Figure 2: Geometry for Image Reconstruction.

as :

$$[Bt](r,\phi) = \int_0^\pi t(r\,cos(\theta - \phi),\theta)\,d\,\theta$$

The back projection operation can be described with reference to Fig. 2. If $P(l,\theta)$, the projection at a given angle θ, is represented as $g_\theta(l)$, then for different distances l from the center, g_θ is a set of projections (line integrals) taken in the θ direction. If the values of $g_\theta(l)$ are backprojected or smeared back over the domain, the resulting function, $b_\theta(x,y)$, at each angle, is given by :

$$b_\theta(x,y) = \int g_\theta(l)\,\delta(x\,cos\theta + y\,\sin\,\theta - l)dl$$

Thus, in the backprojection operation each projection at a point t (Ref. Fig. 2) makes the same contribution to all the pixels along the line l. The complete backprojected function is the sum of all such functions corresponding to all the angles. Hence, the

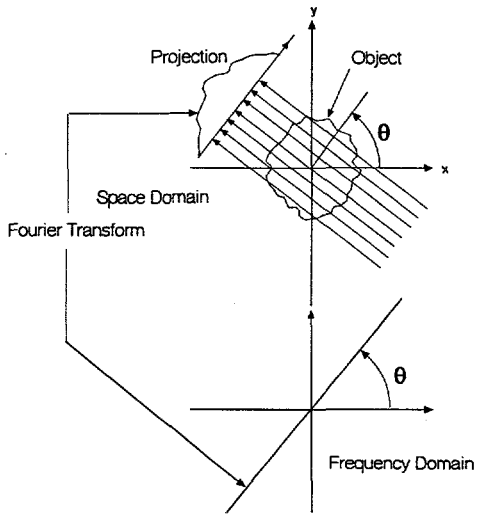

Figure 3: Pictorial representation of the Fourier slice theorem

approximation $f'(x,y)$ to $f(x,y)$ is :

$$\begin{aligned} f'(x,y) &= \int_0^{\pi} b_\theta(x,y)\, d\theta \\ &= \int_0^{\pi} \int g_\theta(l)\, \delta(x\, cos\theta + y\, sin\theta - l) dl \end{aligned} \tag{6}$$

4. The value of $f'(x,y)$ is then normalized by multiplying it by $-1/(2\pi)$.

A very commonly used algorithm for reconstruction in commercial CT scanners is the filtered backprojection, or its equivalent, the convolution backprojection system. The implementation of these algorithms on a computer gets simplified by making use of Fast Fourier Transforms (FFT). With the use of FFT the execution of the algorithm is also faster. The principle basis for these algorithms is the central section theorem (Gordon and Herman, 1974) which states that all the ray sums or the projections in one view of the object constitute the two dimensional sinusoidal components of the unknown image at that angle. Thus, the measured projections at each angle are used to derive the Fourier Transform (FT) of the object at that angle. This, as shown in Fig. 3, constitutes a line in the Fourier plane at the same angle. Repeating this for all the projections then provides the FT of the image of the section being scanned in the form of a series of lines radiating from the center. The reconstruction is then finally obtained by taking the inverse Fourier transform.

Before the inverse FT is computed, the FT in the plane is first multiplied by a band-limited filter function. The purpose of this filtering is to reduce the blurring caused by the

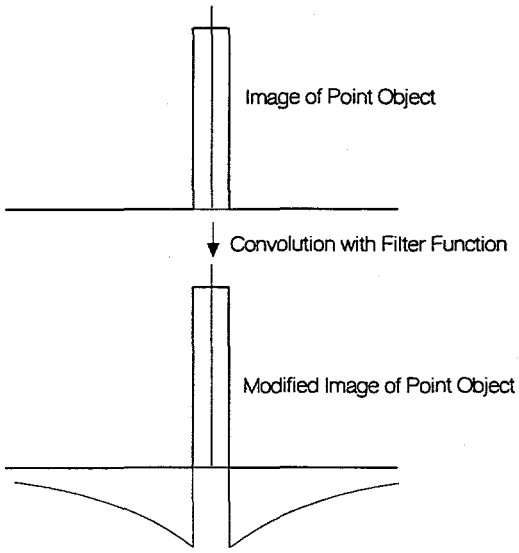

Figure 4: Modification of the image of a point object by a filter function

back-projection process. As the backprojection process leads to a uniform assignment of the projected value along the beam path, the reconstruction of a point object appears as an array of lines or spokes intersecting at the point being reconstructed and therefore the image is not sharp. Since an image is a collection of points, the blurring of the image is a result of the backprojection process. In order to reduce the effects of blurring it is necessary to suitably modify the projections before they are backprojected. Each point is therefore replaced by a modified function as shown in Fig. 4. The modified function has the same amplitude as the point object but includes negative extensions on either side of its position that will cancel out the blurring effect of the backprojection process. The modified function for each point of the image has the same shape but with an amplitude that is a function of the amplitude of the original point. Summation of the modified functions leads to addition and subtraction of the negative and positive parts of the functions leading to the convolved projections. All this is effectively achieved by the multiplication of the FT of the filter function with the FT of the projections in Fourier space. In order to compute the inverse FT of the filtered projections it is also necessary to interpolate the FT of the filtered projections that are known along a finite number of radial lines from a polar grid on to a cartesian grid. Traditionally, either a nearest neighbor or a linear interpolation approach is used. This generally leads to large errors as the radial points get sparser with increase in distance from the center. The end result, caused by this interpolation, is that the high frequency components of the image are in greater error leading to image degradation.

The above description of the reconstruction process holds for the projections measured in

the parallel beam scanning mode. For image reconstruction from the measurements obtained with fan-beam scanning configuration, the general idea provided above is still applicable, but the details of the algorithm derivation differ. The differences arise mainly because of the different mathematical expression that arise in the algorithm derivation process. Consequently, the filter used is different, and instead of a simple backprojection, as used for parallel beams, it is necessary to implement a weighted backprojection. Details of the algorithm as well as the implementation on a computer can be found in Herman et al. (1976). Another approach that is used for reconstructing fan beam projections is to first convert the fan-beam data to equivalent parallel beam projection measurements by a method known as rebining (Dreike & Boyd, 1976). The rebined data are then reconstructed using the parallel beam algorithm. Algorithms based on these principles are most commonly used in present day medical scanners since, being noniterative, they involve relatively fewer computations and are less susceptible to noise. In addition, each set of projections can be processed immediately as they are acquired. The latter feature is important in the medical field because of the necessity of on-line diagnosis of the patient's condition.

Algebraic Reconstruction Techniques (ART) fall under a more general class of algorithms called series expansion methods (Gordon, 1974). These methods transform the problem of estimating the linear attenuation coefficients to finding a finite set of numbers through the solution of a set of linear algebraic equations. The image is discretized into a finite number of elements called pixels, with the pixels being identified by their row and column numbers i and j, respectively. The value in each pixel is a number proportional to the linear attenuation coefficient within that pixel. The algorithm begins by guessing these numbers $A(i,j)$ for all the pixels, and then modifies each element along each ray by a factor that compensates for the discrepancy between the measured ray sum $P(l,\theta)$ and the calculated ray sum $R(l,\theta)$. Two forms of ART can be differentiated depending upon the method used for correcting the pixel values. In additive ART the correction is based on :

$$A^{n+1}(i,j) = max\{A^n(i,j) + (P(l,\theta) - R(l,\theta))/N_{(l,\theta)}, 0\} \tag{7}$$

where $N_{(l,\theta)}$ is the number of pixels that lie along the projection under consideration. The multiplicative form of ART uses the expression :

$$A^{n+1}(i,j) = A^n(i,j)\frac{P(l,\theta)}{R(l,\theta)} \tag{8}$$

If the calculated ray sum is the same as the measured one, then the assumed values are taken to be the correct ones for that projection. However, if for some other projection there is a large error, then the picture elements of the last projection which lie in the ray for a

new projection are modified as required by the discrepancy between the calculated and the measured value. Thus, each projection in each view is examined and values of $A(i,j)$ are changed in an iterative manner. These algorithms require relatively more computations and are susceptible to noise. In return, they are more tolerant to missing data and allow the incorporation of a priori information or constraints.

An algorithm which has found extensive application in emission tomography is the Estimation-Maximization (EM) algorithm. It is based on an exact stochastic model of projection measurements (Dempster et al., 1977) and is an iterative, algebraic technique used to find maximum likelihood estimates from incomplete data. The measured projections are considered to be incomplete data, in the sense that no measurement is completely representative of the system being investigated. Two sample spaces X, and Y, are defined with the observed incomplete data $y \subseteq Y$ having a probability density function $g(y,\theta)$ (either known or assumed), where θ is a vector of parameters to be estimated. The data that one would ideally obtain is referred to as complete data $x \subseteq X$ and is related to y through a mapping $h : X \rightarrow Y$ such that $h(x) = y$. The postulate is that the incomplete data is a subset of the complete (unobserved) data. The criteria for defining the complete data space is based on the physics of the problem. If x has a probability density function $f(x,\theta)$ then

$$g(y,\theta) = \int_{\{x:h(x)=y\}} f(x,\theta)dx \tag{9}$$

x being determined by $y = y(x)$.

The E-M algorithm aims at finding θ which maximizes $g(y,\theta)$ using the density function $f(x,\theta)$. The estimation or the **E** step consists of forming the conditional expectation $E\left(ln\, f(x,\theta) \,|\, y,\theta^n\right)$, where θ^n represents the current estimate of the vector of parameters. The maximization, or the **M** step, chooses θ^{n+1} as the new vector estimate which maximizes the conditional expectation. The new estimate is then used in the **E** step and the process is repeated until the logarithm of the likelihood function, $ln\; g(y,\theta)$ is maximized. A comprehensive discussion of the E-M algorithm has been presented by Dempster et al. (1977).

Some of the merits of this algorithm are that it can account for statistical variations, can easily incorporate effects of nonuniform beams and other pathological effects. There is also no need for rebining the fan beam data into parallel beams, and the non-negativity of the final reconstruction is assured. The adaptation of this algorithm to transmission tomography was first accomplished by Lange and Carson (1984). Another advantage in comparison to the transform method based algorithms lies in the implementation. The mechanics of the algorithm do not change in accordance with the geometry of data collection. However, the algorithm does need information to be generated for the geometry of the reconstruction,

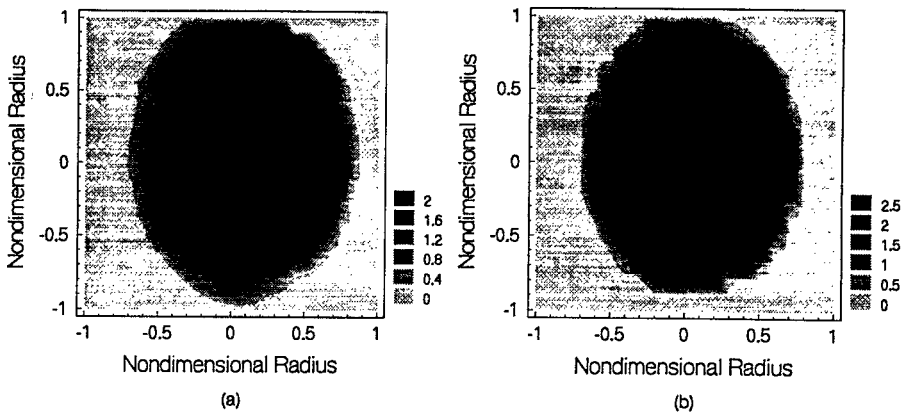

Figure 5: Comparison of reconstruction of a phantom using filtered backprojection and the E-M algorithm.

such as the identity of the pixels that intersect each beam in each view as well as the length of intersection of the beams with each of those pixels.

We have tested the capabilities of the above algorithms for image reconstruction on both simulated as well as measured projections of a number of static density distributions. Objects for testing the reconstruction accuracy of the algorithms, or the imaging capabilities of tomographic scanners, are referred to as phantoms. For comparing the accuracy of reconstruction of the filtered back-projection and the E-M algorithm, the parallel beam projections for an ellipse with a uniform attenuation coefficient of 2 density units were simulated. The number of views simulated were 45 over 180° and the number of beams in one view were 24. The major and minor axis of the ellipse was 0.96 and 0.62 length units, respectively. The region of reconstruction was subdivided into 24 $\times$ 24 pixels leading to a spatial resolution of 0.0833 length units. Ideal conditions are assumed so that there is no noise included in the simulated projection measurements. The Filtered Back Projection algorithm for parallel beam geometry and the E-M algorithm were implemented as part of the development of a CT scanner in our laboratory. Figures 5 (a) and (b) illustrate the reconstruction obtained by Filtered Back Projection and the EM algorithm, respectively. The expected reconstruction is an image of an ellipse with pixels indicating an attenuation coefficient close to 2.0. With the reconstruction made by using the Filtered Backprojection there is what is referred to as the cupping artifact (the lower densities in the middle). With the reconstruction made by the E-M algorithm there is uniformity in the reconstructed value in the pixels with the magnitudes ranging from 1.8 to 2.1.

The reconstruction capabilities of the algorithms are also assessed by comparing the images reconstructed from the projections measured for an actual phantom using the CT scanner in our laboratory. A description of the CT scanner and its capabilities is deferred

to a later section of the chapter. The transmission data for a plexiglas column of 0.19 m internal diameter filled with water was acquired over 90 views with 39 projections each. It has to be noted that the water in the column is static (no flow). The image was reconstructed via the Snark89 (Herman et al., 1989) image reconstruction package using the convolution method for divergent beam projection data as well as by an additive algebraic reconstruction algorithm (ART). These are compared with the image reconstructed by the E-M algorithm in Fig. 6. The reconstructed number in each pixel should ideally be $0.086\,cm^2/g$, corresponding to the mass attenuation coefficient of water at 660 keV which is the peak energy of the radiation from the Cs-137 radiation source used in the scanner. Although visually the

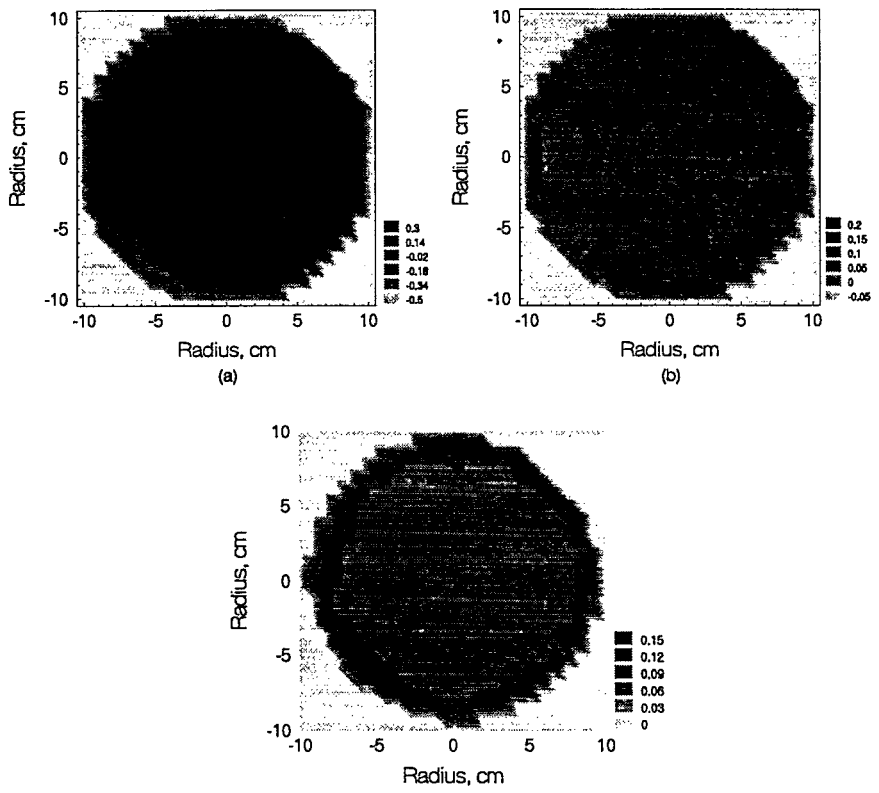

Figure 6: Comparison of reconstructions from different algorithms, (a) Convolution-Backprojection, (b) Additive ART, (c) E-M algorithm.

reconstruction by the convolution method appears to be better, quantitative comparison between the reconstructions has to be made on the basis of the magnitudes assigned to the color bar. The mean attenuation coefficient, and the deviation from the mean, obtained using the three algorithms are reported in Table 2.3. The mean reconstructed value obtained using the traditionally used algorithms are far away from the desired value of $0.086\,cm^2/g$

and the spread in the pixel values is much larger. The uniformity of the reconstruction by the E-M algorithm can be judged on the basis of the corresponding numbers in the table.

Table 1: Mean and standard deviation of attenuation coefficients reconstructed by the three algorithms

Algorithm	Reconstructed Mean	Std. Dev.
Convolution	0.0736	0.060
ART	0.0728	0.030
E-M Algorithm	0.0887	0.003

3 Hardware Elements for a CT Scanner

The two primary elements of a CT scanner are the radiation detectors and the source of radiation. There are two main types of detectors, the classification depends on the principle used in the detection process. In the detectors of the ionization chamber type, the sensors react to the ionization produced in them by the radiation. In the scintillation type detectors, excitation or molecular dissociation induced by the radiation produces the measured effect. For transmission type CT scanners the scintillation detectors are extensively used. These detectors are actually a combination of a scintillation crystal, a photocathode and a photomultiplier that produces a voltage proportional to the intensity of the incident radiation. These kind of detectors have the capacity to handle count-rates of up to 10^{10} events per second. For steady state measurements thallium activated sodium iodide crystal is commonly used owing to a very high conversion efficiency and a short decay time (10^{-7} s). For transient measurements, however, some organic materials such as anthracene and stilbene are used because of their short recovery times. They, however, have a relatively low conversion efficiency.

The two types of radiation that can be employed in CT scanners are X-rays and gamma rays. Both of them consist of what are referred to as photons which are packets (quantum) of electromagnetic radiation with neither charge nor mass. Hence, X-rays and gamma rays are physically identical differing only in their origin. X-rays result from the bombardment of a target with high speed electrons and, therefore, X-ray machines are essentially electron accelerators. A high energy electron beam is converted into X-rays by making use of a suitable target material. The efficiency of this conversion process is low being of the order of 10% or less. The characteristics of the X-ray energy depends on the nature of the target

material used in the X-ray tube. Tungsten and molybdenum are the most commonly used target materials. Since the mass absorption coefficient for an X-ray is inversely proportional to the one-third power of the X-ray energy, a suitable choice of the energy is required to obtain optimum attenuation of the X-ray beam. The following table lists the transmittance i. e. the fraction of the initial intensity that emerges without attenuation for an X-ray beam at different energy levels.

Table 2: Transmittance of X-ray at different energy levels

Energy - keV	Depth of water - cm	
	1.0	0.1
5	0.017	0.66
6	0.087	0.78
8	0.34	0.90
10	0.56	0.94

Most often the characteristic energy of the photons emerging out of an X-ray tube are relatively low. At low energies the proportion of the photons that are removed from the beam is higher. A 1 cm thick steel specimen will attenuate the intensity to only about 10 % of the initial intensity at 100 keV, 30 % at 200 keV and 50 % at 500 keV. In order to be able to study large test sections it then becomes necessary to have photons of higher characteristic energy. Radioisotopes that emit gamma rays typically have higher characteristic energy and are to be preferred over X-ray tubes for process engineering tomography.

The number of photons emitted by a radioisotope is proportional to the number of disintegrations. This decay rate is usually expressed in Curies which is equivalent to 3.7×10^{10} disintegrations per second. Since the emission of radiation from radioisotopes is isotropic, only a fraction of the disintegrations can be used for measurement purposes. A typical solid angle factor is 10^{-5}. With the use of collimation for the source as well as for the detectors in CT scanners, the number of photons that could be available is further reduced. There are two types of radioisotopes that can be used as a source of gamma radiation. These are the separated fission products, such as Cesium-137, and isotopes that are made active by neutron bombardment. Most often the cost of the former type of sources tends to be high and, depending on the application, the latter type of isotopes are more commonly used. The choice of the source strength depends on the application and the accuracy desired. If steady state measurements are adequate, then strengths in the millicurie range suffice. However, if transient measurements in process systems of a couple of feet in diameter are required, then source strengths of at least 5 Curies might be necessary. This amount of radioactivity can

raise serious safety considerations, and extensive measures for handling such a system would have to be incorporated in the facility. The choice of a particular isotope also depends on its half-life, the decay pattern, and also the photon energy and its distribution. A reasonably long half-life period is desirable in order to avoid frequent recalibrations due to decay in source strength. The decay pattern of the isotope needs to be considered for evaluating the ratio of beta to gamma radiation as well as for the determination of the properties of the associated secondary radiation. The peak energy of the photons should be high enough to give a not too small value of the transmission ratio I/I_o. It is also desirable that the distribution of the photon energies be unimodal and as narrow as possible. This reduces the effects of polychromaticity of the beam and the beam hardening artifacts in the final reconstructed image.

In addition to the source and the detectors, the other hardware required for a CT scanner consists of : collimators, the positioning system for orienting the source-detector assembly with respect to the system being imaged, the data acquisition and signal processing system, and a host computer. Medical CT scanners are designed for imaging the internals of the human body. Thus, the orientation of these scanners is such that the imaging process can be carried out when the person is lying down. In process systems most often the test sections of interest are vertical, and, consequently, medical scanners with the design mentioned above are not suitable for use. Scanners for use in process engineering applications are typically designed in house. Therefore, the hardware, as well as the associated signal processing and data acquisition system, for the CT scanner that was developed in the our laboratory serves as an example and is described below.

3.1 The CT Scanner at CREL

CT scanners with the fourth generation scanning configuration (fixed detector-rotating source) are capable of providing temporal resolution of the order of seconds. The hardware for such a scanner is simpler since it is only the source that rotates. Consequently, the inertia of the system is very low and therefore the demands on the rotary positioning device is not high. However, the detectors in such a scanner cannot be collimated since they have to be able to detect rays from a large number of directions. The probability of scattered radiation corrupting the attenuation measurements is high. In addition, the number of detectors that are required is very large leading to a very expensive system. Therefore, the third generation configuration was adopted for our scanner. In this scanning configuration the entire arrangement of the detectors, source and collimators has to be rotated around the test section. Since the inertia of the system to be moved in this configuration is large, a temporal resolution of the order of a few seconds cannot be expected. A schematic of the scanner developed at the

Chemical Reaction Engineering Laboratory (CREL), Washington University, in St. Louis, is illustrated in Fig. 7.

Central to the unit is the scanning assembly consisting of a rotation stage (gantry) on which an array of eleven scintillation detectors is mounted on one side and a source holder on the opposite side of the test section. The whole assembly of the detectors and the source can be rotated about the axis of the test section through a stepper motor interfaced to a host computer. A resolution of 0.1° can be achieved by the rotary positioning system. Consequently, there is no serious limitation on the number of views that can be obtained to reconstruct the image of the cross section. The optimum number of views required is dictated primarily by the desired density resolution, and increases with the demand for a higher resolution. The source used is an encapsulated 100 mCi Cesium-137 isotope. The encapsulation is such that it provides a fan beam subtending an angle of 40° in the horizontal plane. The source has been further collimated using a 20 × 10 × 10 cm lead brick with a central slit such that the emerging beam has a thickness of 6.5 mm at a distance of 28 cm from the source. This amount of source collimation was required in order to reduce the background counts to less than 5% of the counts measured in air. The detectors used are 2" × 2" NaI scintillation detectors. The arc in which the detectors are set has a radius of 0.923 m. This radius was necessary to accommodate test sections as large as 0.35 m in diameter. Given this radius and the size of the detectors only eleven of them could be accommodated in the fan beam arc of 40°. If one were to use the system in this configuration there would be only eleven chordal transmittance measurements (with the number going down as the size of the test section is reduced) leading not only to a coarse spatial resolution but also to severe aliasing as indicated by signal sampling considerations. The number of detectors in the arc were therefore effectively increased by making use of a collimator, which for a given view moves across the detector arc, so that each detector samples multiple rays. This however, leads to increased scanning time (the scanning time increases in proportion to the number of additional rays sampled by a detector). The movement of the collimator is achieved by another independent stepper motor, also interfaced with the host computer. The collimator made of lead is 6.35 cm deep and has a height of 7.62 cm. The detectors are completely shielded by the collimator. The collimator has rectangular holes 5 × 10 mm at locations appropriate to each of the detectors. These dimensions for the collimator holes were optimized based on considerations of providing adequate area for detecting photons with good statistics in the chosen sampling period. The entire scanning assembly weighs about 90 kgs, and consequently the maximum rotational speed that can be achieved is about 1 r.p.m. This implies that the temporal resolution of the scanner is not adequate for detecting transients in the flow. Adequate care has been taken in choosing gears with

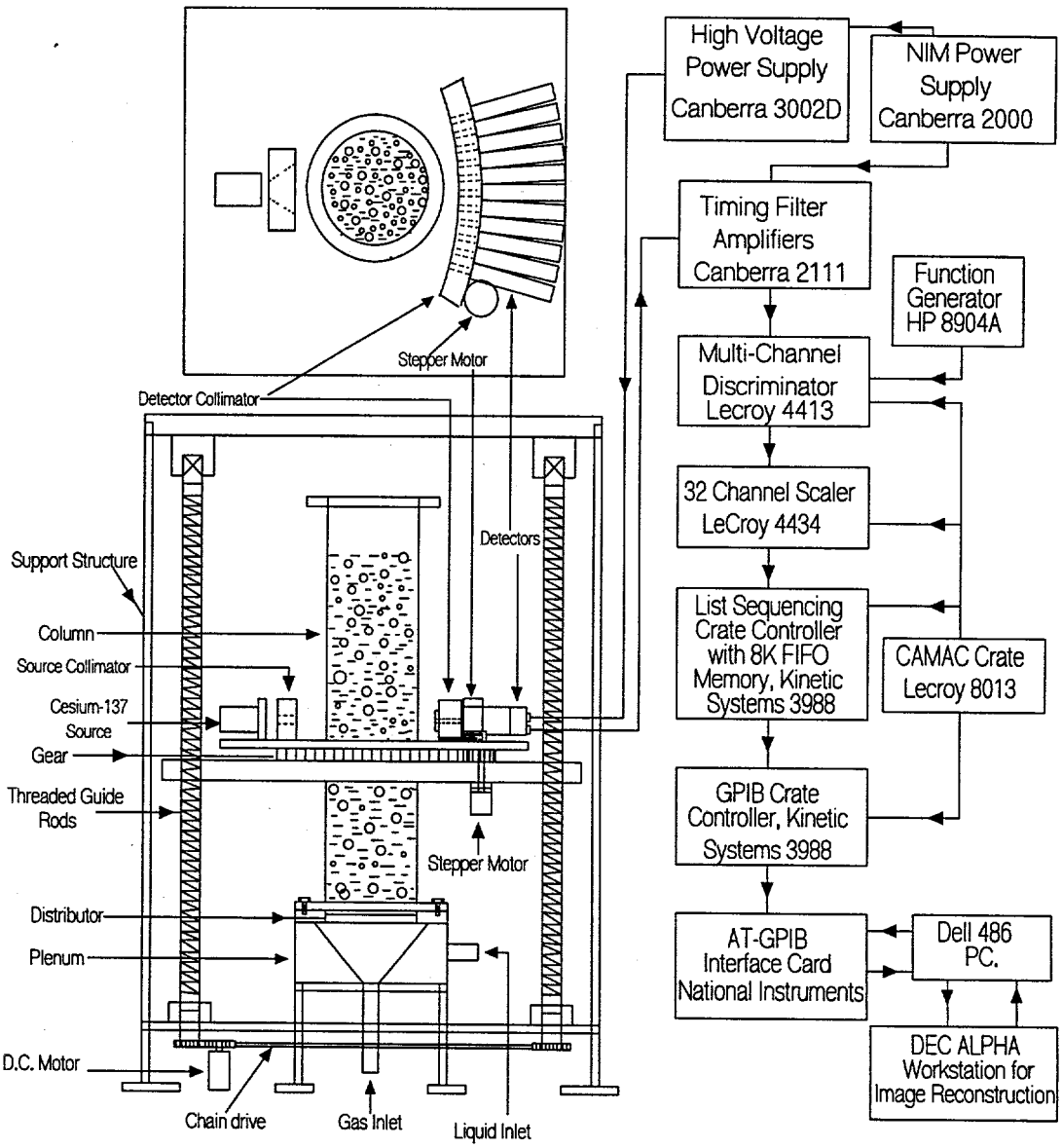

Figure 7: Schematic of the CT Scanner.

negligible backlash so that the motion of the collimator, and that of the scanning assembly as a whole, can be controlled with precision and accuracy. The entire scanning assembly has a central opening large enough for it to translate up and down with respect to the test section. This latter motion is achieved by means of four precision square threaded screws supporting the scanning assembly at the corners. They can be driven synchronously to accomplish the axial positioning required for scanning different horizontal sections of the column. The system also incorporates adequate shielding using lead bricks for radiation safety.

4 The Signal Processing and Data Acquisition System

Gamma photons randomly emitted from the source get attenuated in number proportional to the holdup distribution that the beam encounters as it traverses the test section. Each photon entering the detector crystal produces a light pulse, which is sensed and amplified by a ten stage photomultiplier tube integrated with the detector. The biasing of the cathodes of the detectors (1000 Volts) is provided by two high voltage power supplies (Canberra, Model 3002D). The voltage pulses are amplified using timing filter amplifiers (Canberra 2111). The amplifiers accept positive or negative current pulses from the detectors and deliver output pulses in the range of $\pm$ 5V range. They have independent adjustments for the differential and integral time constants in their RC-CR circuits. These controls enable one to shorten the tail of the signal pulse and to choose a suitable amplitude, respectively. The power to the amplifiers is fed by NIM/BIN power supplies (Canberra 2000). The signals from the amplifiers are fed to discriminators to eliminate undesired secondary emissions. The threshold for the discriminators is continuously adjustable from 15 mV to 1 V either by a potentiometer on the front panel or by software control. A threshold voltage of 45 mV was found to be adequate for removing most of the secondary emissions. Thus, the discriminator produces a logic pulse corresponding only to those photons depositing their full energy in the detector. The logic pulses are counted directly using a multichannel 24 bit scaler (binary counter). The scaler also carries a temporary buffer corresponding to each channel for storing the accumulated counts. A function generator inputs a sine wave at a known frequency to one of the channels of the scaler as a reference input for error control. A list sequencing crate controller with 8K FIFO (first in - first out) memory serves as a buffer when the contents of the scaler are emptied at user specified sampling rates. When the FIFO memory is half full a CAMAC (Computer Automated Measurement and Control) crate controller transfers its contents to the host computer hard disk via a GPIB (General Purpose Interface Bus (IEEE 488)). The transfer from the scaler buffer to the FIFO memory, as well as the transfer from

the FIFO memory to the computer memory and later to the hard disk, proceed in parallel with no data loss. The advantage of using CAMAC instead of A/D converters is that it allows a wide range of modular instruments to be interfaced to a standardized crate. The crate has a dataway that provides a pathway between the modules and a host computer. The crate has a number of stations in which different modules (such as scalers, discriminators etc.) can be inserted. The last two stations of the crate are meant for crate controllers whose purpose is to issue commands to the modules and also transfer information between the modules and the host computer.

Also embedded in the acquisition process is the control of the motion of the stepper motors required for the positioning of the collimator (for obtaining different rays in a given view) and the scanning assembly as a whole (for obtaining different views). The two stepper motors (Superior Electric, M092-FD-8009) have independent indexers (Superior Electric Model 430-PT) that are interfaced to the host computer using RS232 communication. All the motion control commands are loaded into the memory of the indexers. Upon receiving a signal issued by the computer at the appropriate instants of time, that are coded into the data acquisition program, the stepper motors induce the required motions. Thus, the entire process of acquiring all the data required for the imaging of a cross section is completely automated.